INTERNATIONAL JOURNAL OF PRECISION ENGINEERING AND MANUFACTURING Vol. 19, No. 10, pp. 1457-1466 OCTOBER 2018 / 1457

REGULAR PAPER

DOI: 10.1007/s12541-018-0172-2
ISSN 2234-7593 (Print) / 2005-4602 (Online)

Dynamic Accuracy Improvement of a MEMS AHRS for Small UAVs

Min-Shik Roh[1] and **Beom-Soo Kang**[1,#]

1 Department of Aerospace Engineering, Pusan National University, 2, Busandehak-ro 63beon-gil, Geumjeong-gu, Busan, 46241, Republic of Korea
Corresponding Author / E-mail: bskang@pusan.ac.kr, TEL: +82-51-510-2310
ORCID: 0000-0003-2649-6166

KEYWORDS: AHRS, UAV, Kalman-filter, Dynamic accuracy

Nowadays, unmanned aerial vehicles are widely used for various applications, with their sizes progressively decreasing as avionics are miniaturized. The development of microelectromechanical system (MEMS) technology has enabled miniaturization of avionics via application of the MEMS inertial measurement unit (IMU) to navigation sensors such as the attitude heading reference system (AHRS). However, perturbation or acceleration is known to cause low accuracy in the MEMS AHRS, which incorporates a critical sensor. Thus, in this paper, a method is proposed to improve the dynamic accuracy of a MEMS AHRS when an aircraft accelerates. The attitude calculations implement a quaternion method. The attitude correction of the AHRS algorithm entails the use of a Kalman filter, which is modified to improve the dynamic accuracy of the AHRS by adjusting the measurement noise covariance of the filter to change according to the maneuvering condition. The performance of the proposed algorithm was evaluated via simulation. For the simulation, actual flight data were acquired via a storage device that synchronizes the output of the reference sensor — a GPS-aided AHRS — and the IMU. Simulation of the proposed algorithm demonstrates that the proposed attitude estimation method yields results that are similar to the output of the reference sensor.

Manuscript received: May 14, 2018 / Revised: July 13, 2018 / Accepted: August 3, 2018

1. Introduction

Unmanned aerial vehicles (UAVs) are aircrafts which perform missions either remotely or autonomous with no onboard pilot. In order to smoothly accomplish a given mission, specific navigation information, such as position, speed, and attitude are required. Accurate attitude information is particularly critical for aircraft control, because many types of aircraft use attitude regulation to modify their flight path and position. Most UAVs are relatively small in size; thus, they require small and lightweight attitude sensors to facilitate the efficiency of devices with minimal space and payload.[1]

The strapdown navigation system is smaller and lighter than the gimbal navigation system; these features make it suitable for small UAVs with small payloads for mission equipment. Because of recent developments in computing and microelectromechanical system (MEMS) technology, sensors have decreased in size and their dynamic range has widened;[2-5] consequently, the development of miniature strapdown navigation sensors was realized. However, because the accuracy of the MEMS gyro is less than that of the gimbal gyro, the MEMS inertial measurement unit (IMU)-equipped attitude heading reference system (AHRS) is strongly influenced by the measurement values of the accelerometer and magnetometer.[6] Thus, although the attitude of the MEMS AHRS may be comparable to the actual attitude for instantaneous acceleration of the aircraft, the attitude error tends to increase when the aircraft accelerates for more than a few seconds.[6]

The aim of this study is to improve the dynamic accuracy of the AHRS during aircraft acceleration. The attitude calculations for the proposed AHRS implement a quaternion-based-method that avoids singularities and facilitates preservation of orthogonality.[7,8] Specific force and earth magnetic field measurements were used to compensate for the accumulated errors in attitude calculations. Additionally, the Kalman filter was modified for use as an attitude compensation algorithm. By designing the measurement noise covariance of the Kalman filter to vary according to the measured acceleration, the dynamic accuracy of the AHRS was found to have improved as compared to the accuracy resulting from the conventional method of implementing a constant measurement noise covariance.

The performance of the designed algorithm was evaluated by comparing the outputs of the reference sensor (a GPS-aided AHRS), the proposed algorithm, and the algorithm with constant measurement

noise covariance. The attitude output of the GPS-aided AHRS is more accurate than that of the MEMS-AHRS because it performs better attitude correction based on the information obtained from the integrated GPS. However, the simulation results show that the proposed method yields better performance than that resulting from implementation of the Kalman filter with constant measurement noise covariance. Moreover, the results of implementing the proposed dynamic accuracy improvement method are comparable to the corresponding results observed via the attitude output of the reference sensor.

2. Attitude Calculation

2.1 Initial attitude determination

Initial attitude determination is the process of calculating the initial rotation angle by transforming the navigation coordinates to body coordinates. Because the platform attitude is calculated by integrating the angular velocity, an initial attitude determination is necessary. In this study, the gravitational and magnetic field were used to determine the initial attitude via the triad algorithm.[9-13] triad algorithm is one of the simplest solutions to the wahba's problem. Wahba's problem is analytical method to find rotation matrix between two coordinate system from a set of vectors.[12-15] the ned coordinate system was used; additionally, because the system model can be simplified via calculation and correction of the attitude, magnetic north was selected as the n axis instead of true north. The triad algorithm determines attitude as based on the relationship between two non-parallel vectors. Triad algorithm is below.[9,10,12,13]

$$g_n = C_b^n g_b , \tag{1}$$

$$m_n = C_b^n m_b , \tag{2}$$

Where C_b^n is the transformation matrix from the body coordinate system to the navigation coordinate system, g is gravitational acceleration, and m is the magnetic field of the earth. Subscript n refers to the navigation coordinate system, and subscript b refers to the body coordinate system.

When the UAV is in non-accelerated state, specific force f_b and gravitational acceleration g_b are equal:[16]

$$g_b = f_b , \tag{3}$$

The following equations describe the process of calculating an orthonormal matrix from geomagnetic and specific forces affecting the body coordinates:

$$r_1 = \frac{f_b}{\|f_b\|} , \tag{4}$$

$$r_2 = \frac{f_b \times m_b}{\|f_b \times m_b\|} , \tag{5}$$

$$r_3 = r_1 \times r_2 , \tag{6}$$

Where r_1, r_2, and r_3 are orthonormal bases vectors. The specific force f_b and geomagnetic field m_b in the body coordinate system are used to obtain r_1, r_2, and r_3.

Similarly, orthonormal bases vectors s_1, s_2, and s_3 are obtained via the gravitational acceleration and geomagnetism in the navigation coordinate system:

$$s_1 = \frac{g_n}{\|g_n\|} , \tag{7}$$

$$s_2 = \frac{g_n \times m_n}{\|g_n \times m_n\|} , \tag{8}$$

$$s_3 = s_1 \times s_2 , \tag{9}$$

Where

$$s_i = C_b^n r_i \qquad (i = 1,2,3), \tag{10}$$

And m_{ref} and m_{mea} are defined as

$$M_{ref} = \begin{bmatrix} s_1 & s_2 & s_3 \end{bmatrix}, \tag{11}$$

$$M_{mea} = \begin{bmatrix} r_1 & r_2 & r_3 \end{bmatrix}, \tag{12}$$

Then,

$$M_{ref} = C_b^n M_{mea} , \tag{13}$$

Because m_{ref} and m_{mea} are both orthonormal matrices,

$$C_b^n = M_{ref} M_{mea}^T , \tag{14}$$

Where

$$C_b^n = \begin{bmatrix} C_{11} & C_{12} & C_{13} \\ C_{21} & C_{22} & C_{23} \\ C_{31} & C_{32} & C_{33} \end{bmatrix}, \tag{15}$$

The initial value of the quaternion can be obtained via the rotation transformation matrix:[17]

$$q_0 = \frac{1}{2}\sqrt{1 + C_{11} + C_{22} + C_{33}} , \tag{16}$$

$$q_1 = \frac{1}{4q_0}(C_{32} + C_{23}), \tag{17}$$

$$q_2 = \frac{1}{4q_0}(C_{13} + C_{31}), \tag{18}$$

$$q_3 = \frac{1}{4q_0}(C_{13} + C_{31}), \tag{19}$$

Where q_0 is scalar, and q_1, q_2, and q_3 are vectors.

2.2 Attitude calculation

The direction cosine matrix (DCM) algorithm, Euler angle algorithm, and quaternion algorithm are the most commonly used attitude calculation algorithms. The Euler angle algorithm is the simplest of these three algorithms. However, it introduces singularities at certain attitudes and requires a relatively large amount of CPU

resources to solve the nonlinear differential equation involving trigonometric functions. Although the DCM algorithm has no singularities, it is relatively time expensive because nine differential equations must be solved. Furthermore, the orthogonality of the transformation matrix may be lost as a result of an accumulation of errors in the solution of the differential equations.[7,8,17-20]

In this paper, a quaternion-based attitude calculation method is used because it has no singularities and requires few calculations, as only four differential equations are solved; this method also facilitates the preservation of orthogonality. To obtain the attitude using a quaternion, the differential equation below must be solved.[17,18] The relationship between the quaternion at the previous time step *k*-1 and the quaternion at the current time step *k* is[17,18,21]

$$q_k = F_k q_{k-1}, \tag{20}$$

where

$$F_k = \cos\frac{\sigma}{2} I + \frac{\sin\frac{\sigma}{2}}{\sigma}\Sigma, \tag{21}$$

and σ represents the rotation angle for a time step; σ and Σ, are respectively obtained as follows:

$$\sigma = \sqrt{\sigma_x^2 + \sigma_y^2 + \sigma_z^2}, \tag{22}$$

$$\Sigma = \begin{bmatrix} 0 & -\sigma_x & -\sigma_y & -\sigma_z \\ \sigma_x & 0 & \sigma_z & -\sigma_y \\ \sigma_y & -\sigma_z & 0 & \sigma_x \\ \sigma_z & \sigma_y & -\sigma_x & 0 \end{bmatrix}. \tag{23}$$

3. Extended Kalman Filter Design

Because AHRSs calculate the attitude by integrating the angular velocity obtained via the gyro to compensate for the accumulation of errors, many types of filters have been proposed and used in AHRSs using gyros and other types of sensors. In this paper, a Kalman filter, which is widely used in engineering, is selected for implementation as an attitude compensation algorithm.[7,14,19,22-32]

3.1 System model

The Kalman filter state variable is designed to be used as a quaternion; the process function for predicting the state is

$$\tilde{x}_k = F_k \hat{x}_{k-1}, \tag{24}$$

where

$$x = \begin{bmatrix} q_0 & q_1 & q_2 & q_3 \end{bmatrix}^T. \tag{25}$$

The measurement *z* is used to normalize the horizontal component of the geomagnetic field m_{b_n} and the specific force f_{b_n}:

$$z = \begin{bmatrix} f_{b_n} \\ m_{b_n} \end{bmatrix}, \tag{26}$$

where

$$f_{b_n} = \frac{f_b}{\|f_b\|}. \tag{27}$$

Because the geomagnetic field is not parallel to the ground, m_{b_n} can be calculated from the geomagnetic measurement and estimated gravitational acceleration. The process of calculating m_{b_n} is as follows. First, the predicted gravitational acceleration vector is normalized to obtain

$$t_1 = \frac{\tilde{g}_b}{\|\tilde{g}_b\|} = C_n^b \frac{g_n}{\|g_n\|}, \tag{28}$$

where $\tilde{g}_b$ is the predicted gravitational acceleration in the body coordinate system. Next, the unit vector t_2 is calculated as follows:

$$t_2 = \frac{\tilde{g}_b \times m_b}{\|\tilde{g}_b \times m_b\|}. \tag{29}$$

This unit vector is both perpendicular to $\tilde{g}_b$ and m_b, and parallel to the ground. Thus, the vector m_{b_n} is obtained via the cross product of t_1 and t_2, where m_{b_n} is parallel to the magnetic north:

$$m_{b_n} = t_2 \times t_1. \tag{30}$$

The measurement function $h(\tilde{x}_k)$ predicts the gravitational acceleration and geomagnetism in the body coordinate system, and C_n^b is obtained from the predicted quaternion via the time update of the Kalman filter:

$$\tilde{z}_k = h(\tilde{x}_k) = \begin{bmatrix} \tilde{g}_{b_n} \\ \tilde{m}_{b_n} \end{bmatrix}, \tag{31}$$

where $\tilde{g}_{b_n}$ and $\tilde{m}_{b_n}$ are the normalized vectors of the predicted gravity and geomagnetic field, respectively, for the body coordinates, which are given by

$$\tilde{g}_{b_n} = C_n^b \frac{g_n}{\|g_n\|}, \tag{32}$$

$$\tilde{m}_{b_n} = C_n^b \frac{m_{n_{kor}}}{\|m_{n_{kor}}\|}. \tag{33}$$

The rotation transformation matrix can be represented as a quaternion as follows:[12,14,17,24]

$$C_n^b = \begin{bmatrix} q_0^2 + q_1^2 - q_2^2 - q_3^2 & 2(q_1q_2 + q_0q_3) & 2(q_1q_3 - q_0q_2) \\ 2(q_1q_2 - q_0q_3) & q_0^2 - q_1^2 + q_2^2 - q_3^2 & 2(q_2q_3 + q_0q_1) \\ 2(q_1q_3 + q_0q_2) & 2(q_2q_3 - q_0q_1) & q_0^2 - q_1^2 - q_2^2 + q_3^2 \end{bmatrix}. \tag{34}$$

Then, the measurement function $h(\tilde{x}_k)$ can be represented in matrix form as follows:

$$\tilde{z}_k = h(\tilde{x}_k) = H_k \tilde{x}_k, \tag{35}$$

where

$$H_k = \begin{bmatrix} q_0g_N + q_3g_E - q_2g_D & q_1g_N + q_2g_E + q_3g_D & -q_2g_N + q_1g_E - q_0g_D & -q_3g_N + q_0g_E + q_1g_D \\ -q_3g_N + q_0g_E + q_1g_D & q_2g_N - q_1g_E + q_0g_D & q_1g_N + q_2g_E + q_3g_D & -q_0g_N - q_3g_E + q_2g_D \\ q_2g_N - q_1g_E + q_0g_D & q_3g_N - q_0g_E - q_1g_D & -q_0g_N + q_3g_E - q_2g_D & q_1g_N + q_2g_E + q_3g_D \\ q_0m_N + q_3m_E - q_2m_D & q_1m_N + q_2m_E + q_3m_D & -q_2m_N + q_1m_E - q_0m_D & -q_3m_N + q_0m_E + q_1m_D \\ -q_3m_N + q_0m_E + q_1m_D & q_2m_N - q_1m_E + q_0m_D & q_1m_N + q_2m_E + q_3m_D & -q_0m_N - q_3m_E + q_2m_D \\ q_2m_N - q_1m_E + q_0m_D & q_3m_N - q_0m_E - q_1m_D & -q_0m_N + q_3m_E - q_2m_D & q_1m_N + q_2m_E + q_3m_D \end{bmatrix}. \tag{36}$$

In Eq. (36), g_N, g_E, and g_D are defined as the components of the normalized gravity vector in the navigation coordinate system:

$$\frac{g_n}{\|g_n\|}=\begin{bmatrix} g_N \\ g_E \\ g_D \end{bmatrix}=\begin{bmatrix} 0 \\ 0 \\ -1 \end{bmatrix}. \tag{37}$$

Magnetic north is defined as north with respect to the navigation coordinate system. Then, the normalized vector of the geomagnetic field vector is given as

$$\frac{m_{n_{hor}}}{\|m_{n_{hor}}\|}=\begin{bmatrix} m_N \\ m_E \\ m_D \end{bmatrix}=\begin{bmatrix} 1 \\ 0 \\ 0 \end{bmatrix}. \tag{38}$$

Substituting Eqs. (37) and (38) into Eq. (36) simplifies the measurement matrix H_k into

$$H_k=\begin{bmatrix} q_2 & -q_3 & q_0 & -q_1 \\ -q_1 & -q_0 & -q_3 & -q_2 \\ -q_0 & q_1 & q_2 & -q_3 \\ q_0 & q_1 & -q_2 & -q_3 \\ -q_3 & q_2 & q_1 & -q_0 \\ q_2 & q_3 & q_0 & q_1 \end{bmatrix}. \tag{39}$$

3.2 Variable measurement noise covariance of kalman filter

The Kalman filter-based system model assumes that the aircraft does not accelerate, and the gravitational acceleration and measured acceleration are equivalent. However, the aircraft accelerates during flight because flight mission profiles include climbing, turning, and descending. This induces a discrepancy between the measured acceleration and gravitational acceleration. Consequently, the error in the attitude estimation model output increases. Dynamic accuracy improvement is expected when the weight of the Kalman filter is adjusted according to information from the acceleration vector.

Because the magnitude of the acceleration acting on a UAV is significantly smaller than that of gravitational acceleration, it is difficult to use it to modify the weight of the algorithm to counterbalance the magnitude of gravitational acceleration. Moreover, the angle between the measured specific force and the predicted gravitational acceleration vector is very sensitive to aircraft acceleration. Therefore, in this paper, a method is proposed to reduce the influence of the UAV's acceleration by designing the Kalman filter to change the measurement noise covariance according to the angle between these two vectors.

Measurement noise covariance R is based on the analysis of noise. However, there are limitations in the analytical determination of R because of the complexity generated by various errors. To overcome this problem, we have empirically determined the measurement noise covariance.[34,35] The simplified measurement noise covariance matrix is

$$R_k=\begin{bmatrix} R_a & 0 & 0 & 0 & 0 & 0 \\ 0 & R_a & 0 & 0 & 0 & 0 \\ 0 & 0 & R_a & 0 & 0 & 0 \\ 0 & 0 & 0 & R_m & 0 & 0 \\ 0 & 0 & 0 & 0 & R_m & 0 \\ 0 & 0 & 0 & 0 & 0 & R_m \end{bmatrix}, \tag{40}$$

where R_a is the measured noise covariance of the acceleration, and R_m refers to the measurement noise covariance of the geomagnetic sensor. When the geomagnetic sensor is well calibrated, R_m is kept constant, as it does not significantly affect the attitude calculation.

The measurement noise covariance of the acceleration R_a is designed to vary according to the magnitude of the angle between the predicted gravitational acceleration and the measured acceleration:

$$R_a=R_{a0}+K_R\alpha\,, \tag{41}$$

$$\alpha=\cos^{-1}\left(\frac{\left(C_n^b g_n\right)\cdot f_b}{\|g_n\|\|f_b\|}\right), \tag{42}$$

where R_{a0} is a constant that is adjusted to yield satisfactory performance when the acceleration is low, and K_R is the weight of angle α. Specifically, α represents the angle between the estimated gravitational acceleration and measured specific force vector. If α is large, then there is a high probability that the aircraft is accelerating; this acceleration generates error in the attitude computation model. Therefore, if the attitude is corrected by f_b when the angle α is large, the attitude error is larger than when there is no acceleration. For this reason, the proposed R_a is designed to reduce the weight of the acceleration measurement value as angle α increases.

Fig. 1 shows the designed algorithm, which is designed to vary the measurement noise covariance R_a of the Kalman filter to improve dynamic accuracy. In Fig. 1, the next quaternion is predicted using ω_b and the previous state value in the attitude calculate block of the time update process. The variable measurement noise covariance block calculates the direction of the gravitational acceleration vector using the predicted quaternion, obtains the acceleration vector at the measured acceleration. And calculates the angle α between the two vectors. R_a increases as the angle alpha increases. The Kalman gain K decreases as R_a increases in the Compute Kalman gain block.

In the Attitude Estimation block, if the Kalman gain K is small, the correction value calculated based on the measured value z is reduced. In this algorithm, assuming acceleration as a disturbance, the weight of the acceleration sensor input is reduced when the aircraft accelerates. So the influence of the disturbance is reduced, consequently, the attitude calculation result is improved.

4. Data Acquisition and Simulation Results

The acquisition data from the flight test was used in the simulation to mimic actual flight conditions. The performance of the proposed algorithm was evaluated by comparing the attitude output of the proposed method to that measured by the reference sensor.

4.1 Data acquisition

The IMU output obtained via the actual flight test was used as input to the simulation to mimic the noise, vibration, and acceleration of the flight conditions of an actual small UAV. The data stored via the data acquisition device are the attitude of the reference sensor and the values of the acceleration, angular velocity, and geomagnetic field measured by the MEMS IMU. Fig. 2 shows the data acquisition device design as a block diagram. The reference sensor used to acquire the data was an NAV-420 (Crossbow Technology, Inc.; Milpitas, CA) as kind of GPS-

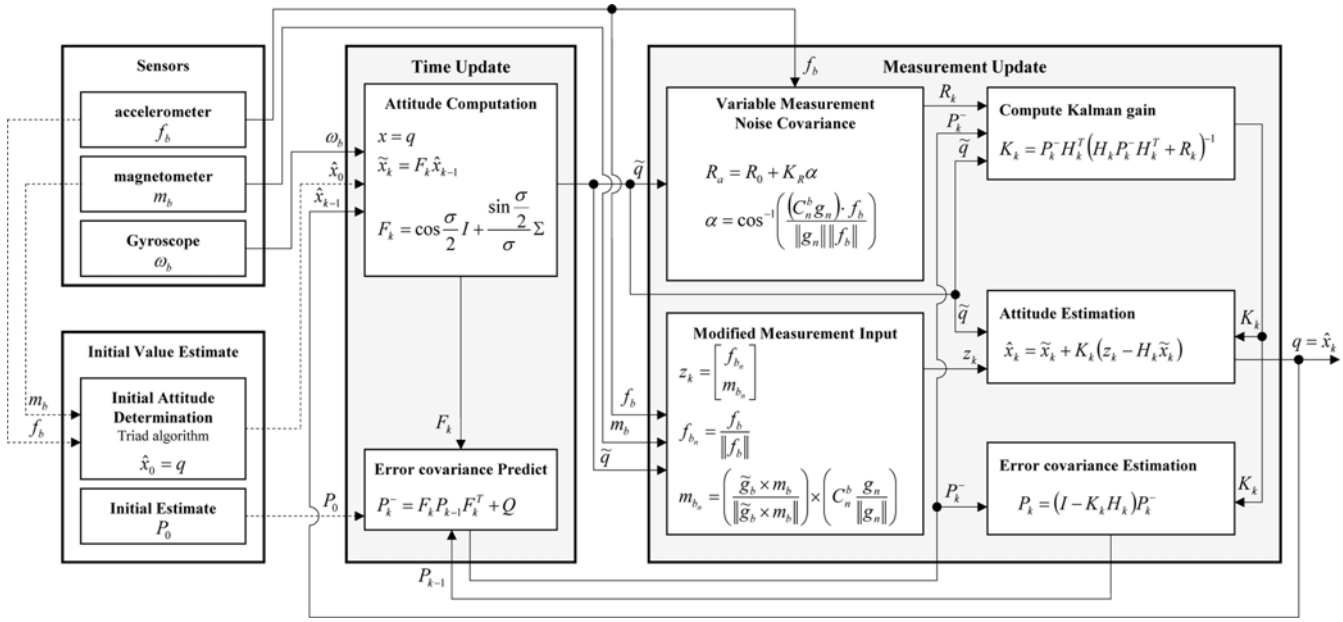

Fig. 1 Block diagram of proposed algorithm

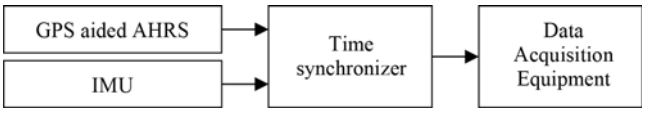

Fig. 2 Block diagram of data acquisition device

aided AHRS, for which performance has been proven on various platforms. The NAV-420 utilizes its integrated GPS receiver to provide more accurate attitude calculation results than the MEMS-AHRS; the ADIS16405 (Analog Devices, Inc.; Livonia, MI) was implemented in the IMU.

The flight test platform was an electric radio-controlled (RC) single-rotor helicopter (Fig. 3), and the skid of the helicopter was modified for installation of a data acquisition device that included an IMU and a reference sensor. The flight scenario entails horizontal acceleration with roll, pitch, and yaw rotation; hovering, was included in the scenario.

4.2 Simulation and results

The data, which includes various maneuvers, comprised 600 seconds of continuous recording during the flight test. These data were subsequently used as input to the simulation. Fig. 4 shows the speed obtained during the flight test via the reference sensor. Each maneuver corresponds to a specific time period in the data, as follows: aircraft take-off at 80 s, hovering from 80 s to ~110 s and 380 s to 525 s, rapid maneuvering from 110 s to 380 s, and landing at 525 s.

The angle α between the predicted gravitational acceleration vector $\tilde{g}_b$ and the measured specific force vector f_b was used to adjust the weight of the Kalman filter and calculated as was described via Eq. (42). The results of this calculation are illustrated in Fig. 5. The measurement noise covariance was varied via the obtained angle α. The constants R_{a0} and K_R were selected to yield satisfactory performance in static and dynamic conditions, respectively. The calculated measurement noise covariance R_a is illustrated in Fig. 6, where R_{a0} is

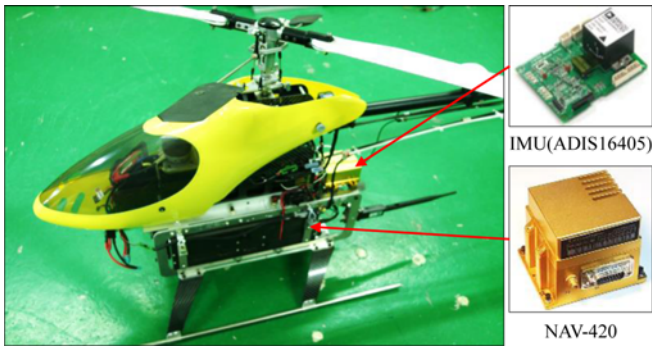

Fig. 3 Single rotor helicopter with data acquisition device

1, and K_R is 7. Figs. 7 and 8 show the attitude angles measured by the reference sensor, and the Euler angles calculated by the proposed algorithm. In these Figs., the solid blue line is the output of the reference sensor, the dashed red line is the output obtained consequent to varying R_a according to the value of α, and the solid yellow line is the output when R_a is kept constant.

Typically, helicopters implement roll and pitch angle regulation to control horizontal acceleration. Fig. 7 shows the results of the simulated roll angle and the output angle of the reference sensor. The period from 310 s to 370 s in the upper graph is enlarged in the lower graph. During this time, the aircraft often maintains a roll angle of over 10° for several seconds and has a high probability of accelerating, as it was found to accelerate relative to the aircraft speed (Fig. 6). In Fig. 7, each time period enclosed within a red dotted circle indicates that the simulation results of the proposed algorithm implementing a variable R_a is more comparable to the reference sensor output than the results of implementing a constant R_a.

The pitch angle results are similarly illustrated in Fig. 8; the time period from 220 s to 280 s in the upper graph is enlarged in the lower graph. The pitch angle results of the proposed algorithm best match the

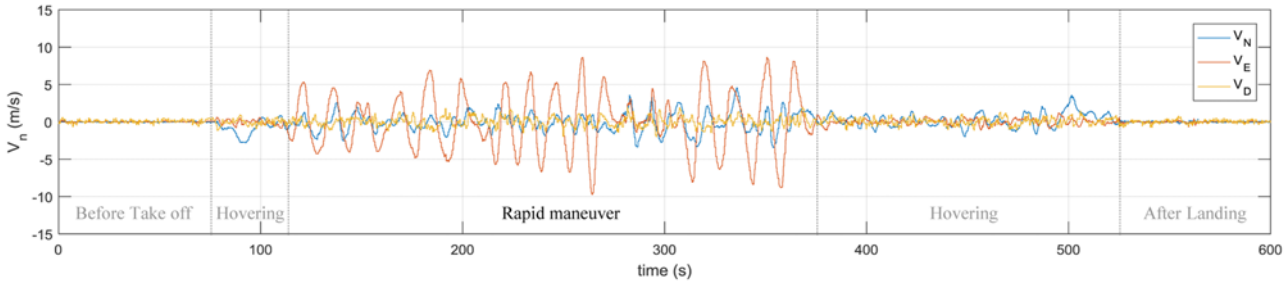

Fig. 4 Velocity

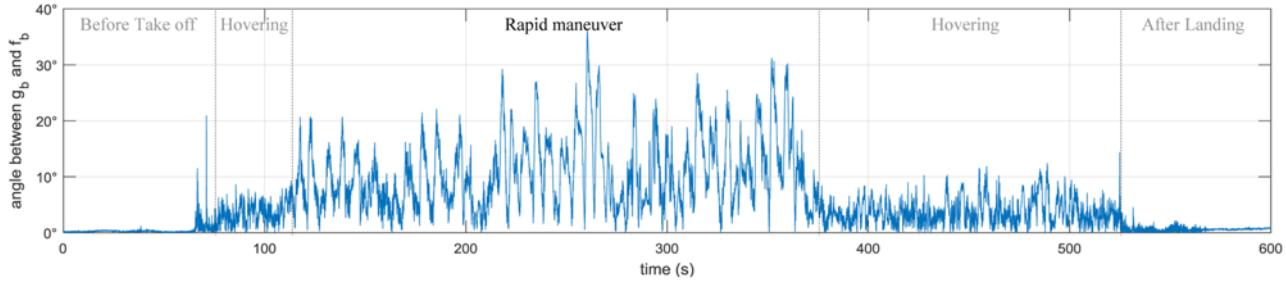

Fig. 5 α angle between two vectors $\tilde{g}_b$ and f_b

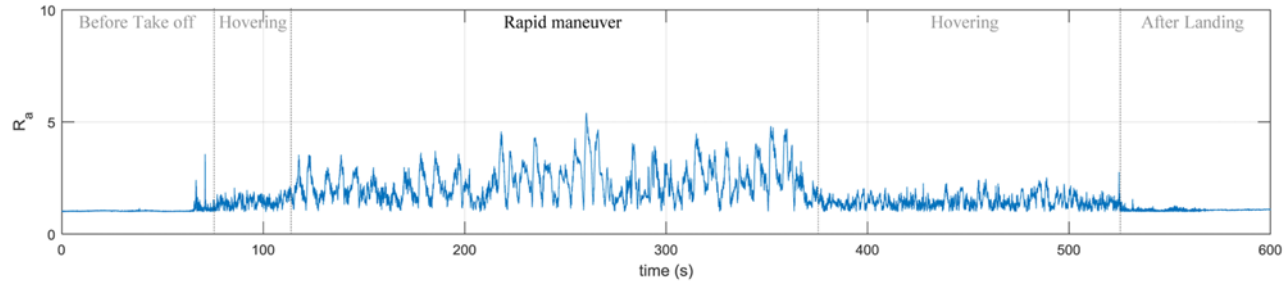

Fig. 6 Calculated measurement noise covariance R_a

reference sensor output during the period of acceleration. This trend is also seen in Figs. 9 and 10, which respectively illustrate the deviation of the roll and pitch attitude angle of the simulated results from those of the reference output. In Figs. 9 and 10, the periods of rapid maneuvering are enclosed within the rounded red boxes; compared to the results of implementing a constant R_a (the yellow line), the variable R_a results (the blue line) remain closer to 0° during rapid maneuvering in the cases of the roll and pitch angles. This means that varying R_a yields results that better mimic the output of the reference sensor.

The standard deviations of the differences between the constant R_a algorithm results and the output of the reference sensor are 0.9° and 0.7° for the roll axis and pitch axis, respectively. In comparison, the standard deviations of the difference between the reference sensor output and the results obtained by using $K_R\alpha$ to vary R_a according to the acceleration of the aircraft are 0.7° and 0.6° for the roll axis and pitch axis, respectively. These results demonstrate that the simulated results obtained by using a variable R_a are more accurate than those obtained by implementing a constant R_a.

Fig. 11 shows the yaw angle output. The proposed algorithm calculates the yaw angle as based on magnetic north, and the reference sensor outputs the angle as based on true north. Thus, there is a difference of approximately 6° to 7° between the results calculated via the algorithm and the reference sensor output. With respect to the yaw axis, the standard deviation of the difference between the reference sensor output and the algorithm output is 1.2° regardless of whether the R_a is variable or constant. Furthermore, the standard deviation with respect to the yaw axis is larger than that with respect to the other axes because the magnetometer measuring the geomagnetic field is sensitive to disturbances. It should be noted that the magnetic disturbance generated by the electric motor of the RC helicopter seems to have influence on the magnetometer of each sensor.

5. Conclusions

In recent years, small, lightweight MEMS strapdown AHRSs have been widely used to ensure compatibility with most UAVs, which are relatively small in size. However, since the accuracy of MEMS gyros are generally low, the attitude calculations of MEMS-AHRSs are strongly influenced by the output of accelerometers and magnetometers

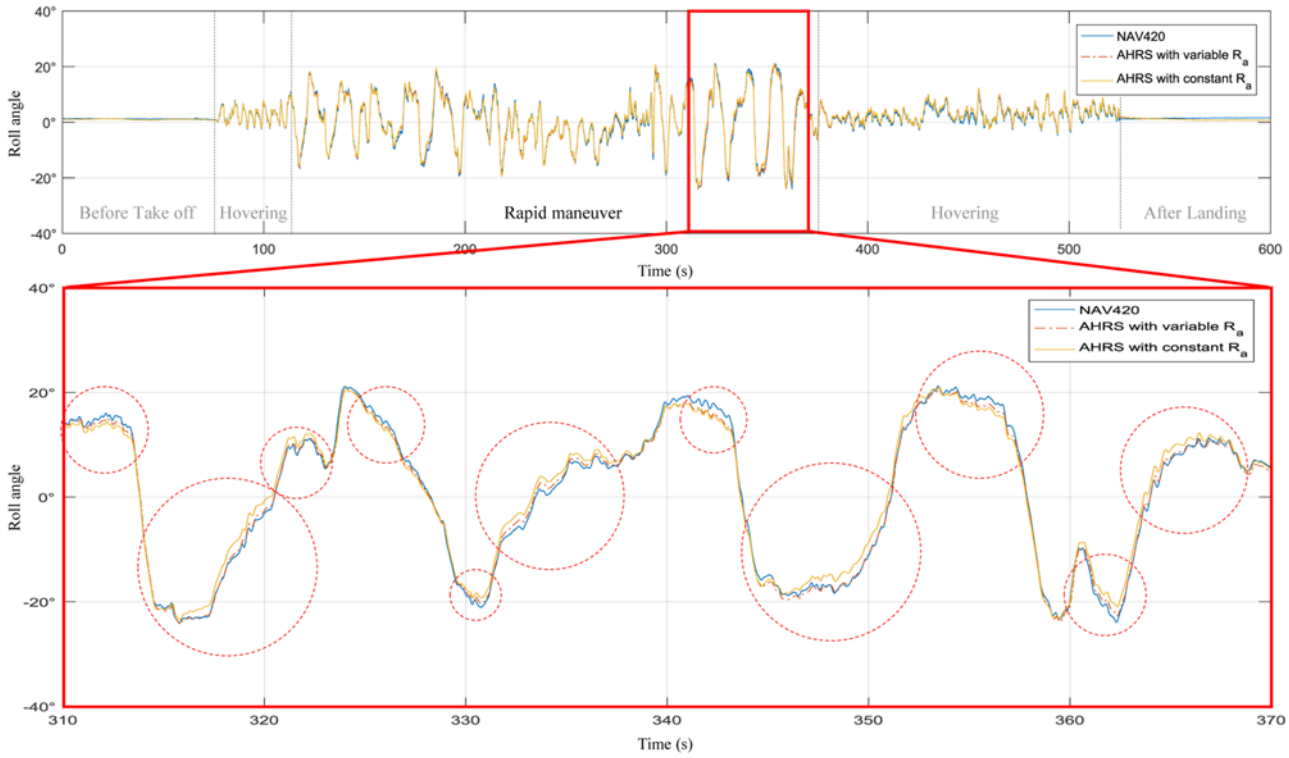

Fig. 7 Roll angle results

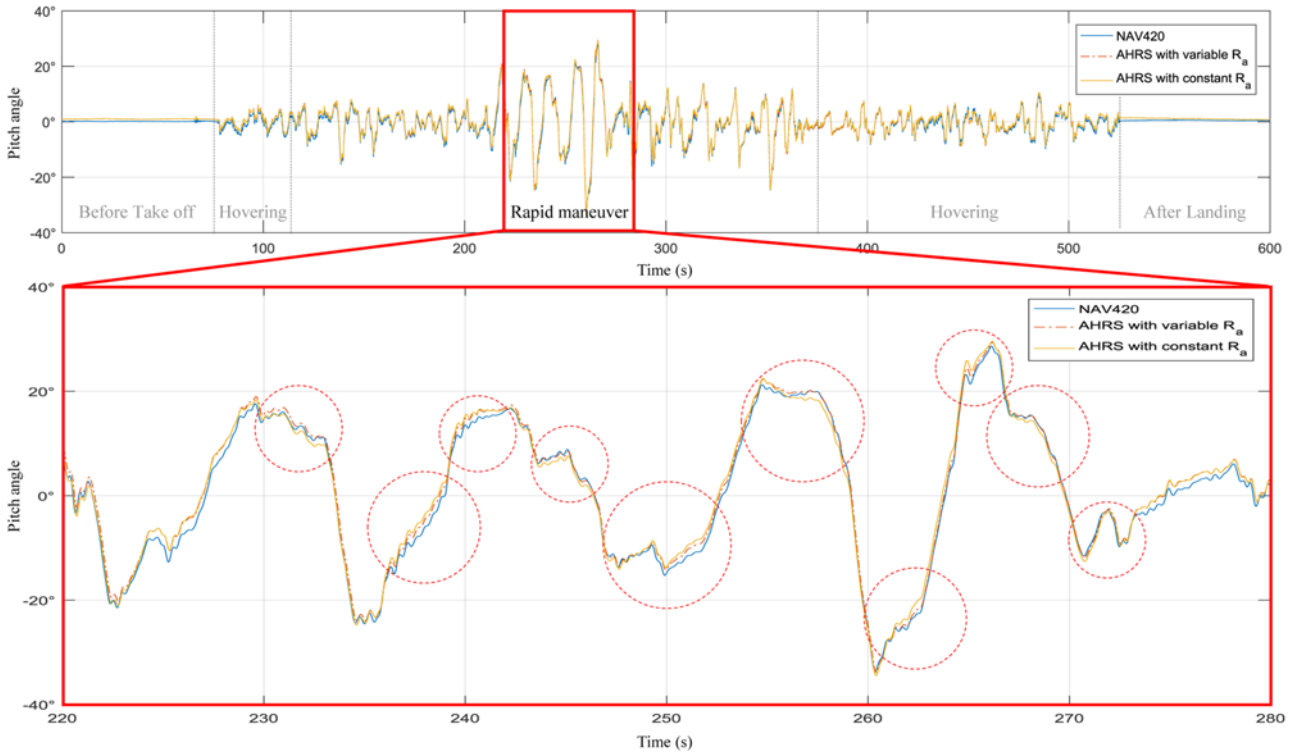

Fig. 8 Pitch angle results

as compared to other types of AHRSs. More specifically, if the acceleration weight generated by the algorithm is large, the attitude error increases when the vehicle accelerates. In this paper, an algorithm was proposed to improve the attitude estimation accuracy under accelerating conditions of an AHRS, and a simulation was performed to verify its performance.

To achieve the aim of improving attitude estimation accuracy, a quaternion-based attitude calculation method was implemented in the

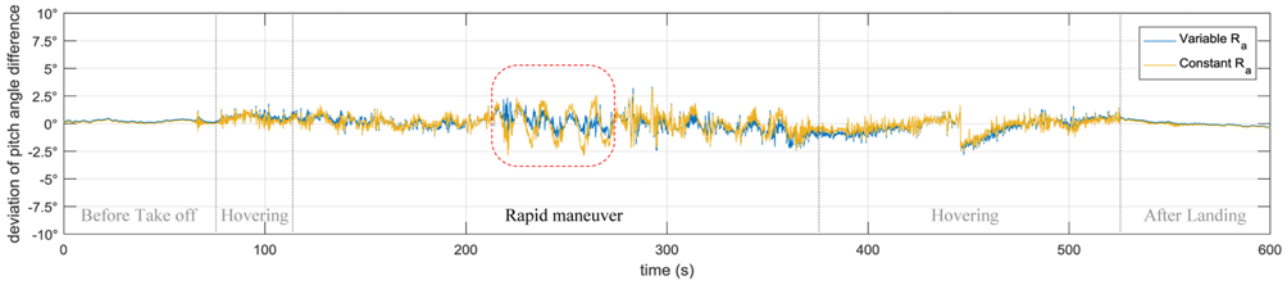

Fig. 9 Deviation of roll angle difference

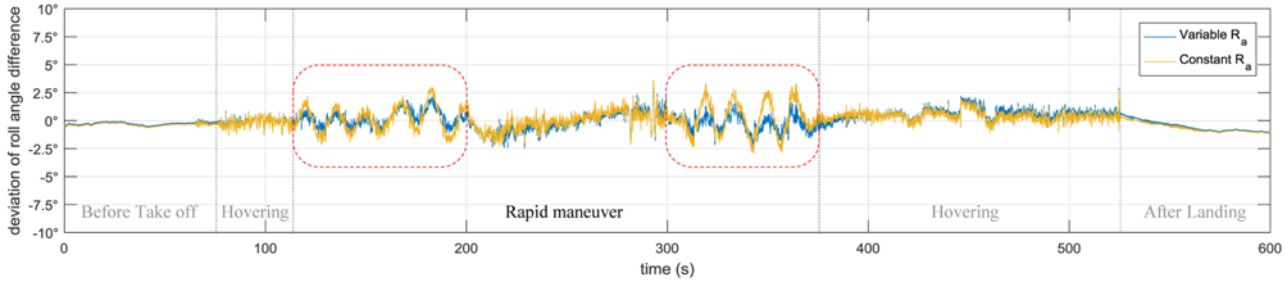

Fig. 10 Deviation of pitch angle difference

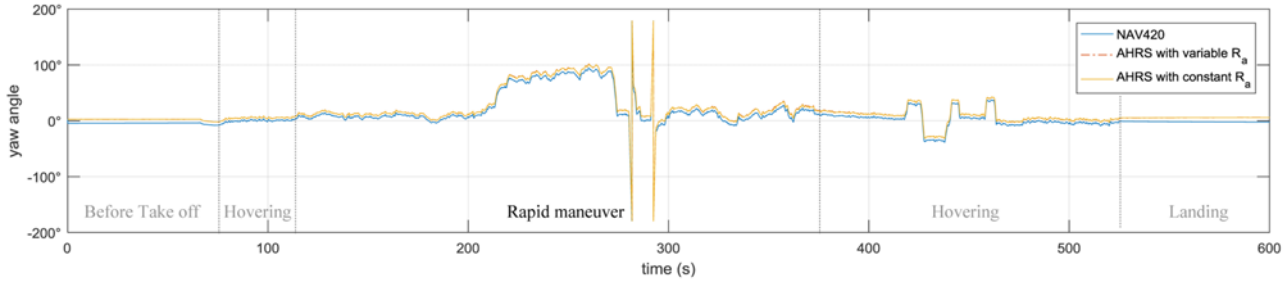

Fig. 11 Yaw angle results

proposed AHRS algorithm. The proposed algorithm offers the advantages of no singularities and relatively simple calculations. An extended Kalman filter was used to derive the algorithm for attitude compensation. In order to improve the dynamic accuracy of the MEMS-AHRS, the measurement noise covariance R_a of the Kalman filter was modified such that R_a varies according to the magnitude of the angle between the gravitational vector and the specific force vector.

In order to mimic actual flight conditions, the output of the IMU obtained from the flight test was used as the input to the algorithm. The output of the IMU and reference sensor (a GPS-aided AHRS) were synchronized and recorded; the performance of the algorithm was evaluated by comparing the results calculated by the proposed algorithm to the output of the reference sensor. The standard deviation of the difference between the angle output of the reference sensor and that of the corresponding simulated result was used as the performance index. A constant R_a yielded a performance index of 0.9° and 0.7° for the roll axis and pitch axis, respectively. Alternatively, varying R_a yielded a performance index of 0.7° and 0.6° for the roll axis and pitch axis, respectively. This means that varying R_a produced a more desirable result for the roll and pitch axes. However, the yaw axis result appeared to be unaffected by the measurement noise covariance of acceleration, as the standard deviation was 1.2° regardless of whether R_a was varied or kept constant.

The results of applying the proposed algorithm to the MEMS IMU-equipped strapdown AHRS are comparable to the output of the reference sensor. In particular, the performance of the proposed algorithm was found to be improved under accelerating conditions. For future research, the proposed algorithm will be implemented in real-time-hardware, and flight testing will be performed to validate the suitability of the proposed AHRS algorithm for actual systems.

ACKNOWLEDGEMENT

This work was supported by the National Research Foundation of Korea (NRF) grant funded by the Korea government (MSIP) through the Engineering Research Center (No. 2012R1A5A1048294).

Also, this work was supported by the Korea Institute for Advancement of Technology (KIAT) grant funded by the Korean government (MOTIE: Ministry of Trade, Industry & Energy) (No. G02N05660000601).

REFERENCES

1. Song, J.-B., Byun, Y.-S., Jeong, J.-S., Kim, J., and Kang, B.-S., "Experimental Study on Cascaded Attitude Angle Control of a Multi-Rotor Unmanned Aerial Vehicle with the Simple Internal Model Control Method," Journal of Mechanical Science and Technology, Vol. 30, No. 11, pp. 5167-5182, 2016.
2. Lee, D., Lee, S., Park, S., and Ko, S., "Test and Error Parameter Estimation for MEMS-Based Low Cost IMU Calibration," International Journal of Precision Engineering and Manufacturing, Vol. 12, No. 4, pp. 597-603, 2011.
3. Lee, J. M., Jang, C. U., Choi, C. J., Kwon, K. B., Han, J. S., et al., "High-Shock Silicon Accelerometer with a Plate Spring," International Journal of Precision Engineering and Manufacturing, Vol. 17, No. 5, pp. 637-644, 2016.
4. Joe, H.-E., Yun, H., Jo, S.-H., Jun, M. B., and Min, B.-K., "A Review on Optical Fiber Sensors for Environmental Monitoring," International Journal of Precision Engineering and Manufacturing-Green Technology, Vol. 5, No. 1, pp. 173-191, 2018.
5. Jeon, T. and Lee, J., "Comparison between Ellipsoid-Fitting Calibration Techniques for Azimuth-Estimating Three-Axis Magnetometer," Journal of the Korean Society for Precision Engineering, Vol. 35, No. 1, pp. 79-85, 2018.
6. Kim, M.-S., Yu, S.-B., and Lee, K.-S., "Development of a High-Precision Calibration Method for Inertial Measurement Unit," International Journal of Precision Engineering and Manufacturing, Vol. 15, No. 3, pp. 567-575, 2014.
7. Qin, F., Chang, L., Jiang, S., and Zha, F., "A Sequential Multiplicative Extended Kalman Filter for Attitude Estimation Using Vector Observations," Sensors (Basel, Switzerland), Vol. 18, No. 5, Paper No. 1414, 2018.
8. Suh, Y. S., "Computationally Efficient Pitch and Roll Estimation Using a Unit Direction Vector," IEEE Transactions on Instrumentation and Measurement, Vol. 67, No. 2, pp. 459-465, 2018.
9. Shuster, M. D. and Oh, S. D., "Three-Axis Attitude Determination from Vector Observations," Journal of Guidance, Control, and Dynamics, Vol. 4, No. 1, pp. 70-77, 1981.
10. Yun, X., Bachmann, E. R., and McGhee, R. B., "A Simplified Quaternion-Based Algorithm for Orientation Estimation from Earth Gravity and Magnetic Field Measurements," IEEE Transactions on Instrumentation and Measurement, Vol. 57, No. 3, pp. 638-650, 2008.
11. Stovner, B. N., Johansen, T. A., Fossen, T. I., and Schjølberg, I., "Attitude Estimation by Multiplicative Exogenous Kalman Filter," Automatica, Vol. 95, pp. 347-355, 2018.
12. Zhu, X., Ma, M., Cheng, D., and Zhou, Z., "An Optimized Triad Algorithm for Attitude Determination," Artificial Satellites, Vol. 52, No. 3, pp. 41-47, 2017.
13. Mohammed, M. S., Bellar, A., Adnane, A., and Boussadia, H., "Performance Analysis of Attitude Determination and Estimation Algorithms Applied to Low Earth Orbit Satellites," Proc. of 11th International Conference on Control (CONTROL), pp. 1-6, 2016.
14. Shan, S., Hou, Z., and Wu, J., "Linear Kalman Filter for Attitude Estimation from Angular Rate and a Single Vector Measurement," Journal of Sensors, Vol. 2017, Article ID: 9560108, 2017.
15. Wu, J., Zhou, Z., Gao, B., Li, R., Cheng, Y., and Fourati, H., "Fast Linear Quaternion Attitude Estimator Using Vector Observations," IEEE Transactions on Automation Science and Engineering, Vol. 15, No. 1, pp. 307-319, 2018.
16. Euston, M., Coote, P., Mahony, R., Kim, J., and Hamel, T., "A Complementary Filter for Attitude Estimation of a Fixed-Wing UAV," Proc. of IEEE/RSJ International Conference on Intelligent Robots and Systems, pp. 340-345, 2008.
17. Titterton, D., Weston, J. L., Weston, J., "Strapdown Inertial Navigation Technology," The Institution of Electrical Engineers, 2004.
18. Ahmed, M. S. and Ćuk, D. V., "Strapdown Attitude Algorithms Using Quaternion Transition Matrix and Random Inputs," Scientific-Technical Review, Vol. 55, No. 1, pp. 3-14, 2005.
19. Ahmed, H. and Tahir, M., "Accurate Attitude Estimation of a Moving Land Vehicle Using Low-Cost MEMS IMU Sensors," IEEE Transactions on Intelligent Transportation Systems, Vol. 18, No. 7, pp. 1723-1739, 2017.
20. Valenti, R. G., Dryanovski, I., and Xiao, J., "Keeping a Good Attitude: A Quaternion-Based Orientation Filter for IMUs and MARGs," Sensors, Vol. 15, No. 8, pp. 19302-19330, 2015.
21. Yuan, X., Yu, S., Zhang, S., Wang, G., and Liu, S., "Quaternion-Based Unscented Kalman Filter for Accurate Indoor Heading Estimation Using Wearable Multi-Sensor System," Sensors, Vol. 15, No. 5, pp. 10872-10890, 2015.
22. Groves, P. D., "Principles of GNSS, Inertial, and Multisensor Integrated Navigation Systems," Artech House, 2013.
23. Chang, L., Zha, F., and Qin, F., "Indirect Kalman Filtering Based Attitude Estimation for Low-Cost Attitude and Heading Reference Systems," IEEE-ASME Transactions on Mechatronics, Vol. 22, No. 4, pp. 1850-1858, 2017.
24. Bishop, G. and Welch, G., "An Introduction to the Kalman Filter," University of North Carolina at Chapel Hill, 2001. (Lesson Course)
25. Vista, F. P., Lee, D.-J., and Chong, K. T., "Design of an EKF-CI Based Sensor Fusion for Robust Heading Estimation of Marine Vehicle," International Journal of Precision Engineering and Manufacturing, Vol. 16, No. 2, pp. 403-407, 2015.
26. Shim, H., Jun, B.-H., Lee, P.-M., and Kim, B., "Dynamic Workspace Control Method for Underwater Manipulator of Floating ROV," International Journal of Precision Engineering and Manufacturing, Vol. 14, No. 3, pp. 387-396, 2013.
27. Jung, D., Seong, J., Moon, C.-B., Jin, J., and Chung, W., "Accurate Calibration of Systematic Errors for Car-Like Mobile Robots Using

Experimental Orientation Errors," International Journal of Precision Engineering and Manufacturing, Vol. 17, No. 9, pp. 1113-1119, 2016.

28. Triwiyanto, T., Wahyunggoro, O., Nugroho, H. A., and Herianto, H., "Evaluating the Performance of Kalman Filter on Elbow Joint Angle Prediction Based on Electromyography," International Journal of Precision Engineering and Manufacturing, Vol. 18, No. 12, pp. 1739-1748, 2017.
29. Seung, J.-H., Atiya, A. F., Parlos, A. G., and Chong, K.-T., "Identification of Unknown Parameter Value for Precise Flow Control of Coupled Tank Using Robust Unscented Kalman Filter," International Journal of Precision Engineering and Manufacturing, Vol. 18, No. 1, pp. 31-38, 2017.
30. Nahian, S. A., Truong, D. Q., Chowdhury, P., Das, D., and Ahn, K. K., "Modeling and Fault Tolerant Control of an Electro-Hydraulic Actuator," International Journal of Precision Engineering and Manufacturing, Vol. 17, No. 10, pp. 1285-1297, 2016.
31. Lee, W., Lee, C.-Y., and Min, B.-K., "Simulation-Based Energy Usage Profiling of Machine Tool at the Component Level," International Journal of Precision Engineering and Manufacturing-Green Technology, Vol. 1, No. 3, pp. 183-189, 2014.
32. Lim, J. and Kang, S., "Non-Inertial Sensor-Based Outdoor Localization for Practical Application of Guide Robots," Journal of the Korean Society for Precision Engineering, Vol. 34, No. 5, pp. 315-321, 2017.
33. Soken, H. E., Hajiyev, C., and Sakai, S.-I., "Robust Kalman Filtering for Small Satellite Attitude Estimation in the Presence of Measurement Faults," European Journal of Control, Vol. 20, No. 2, pp. 64-72, 2014.
34. Christophersen, H. B., Pickell, R. W., Neidhoefer, J. C., Koller, A. A., Kannan, S. K., and Johnson, E. N., "A Compact Guidance, Navigation, and Control System for Unmanned Aerial Vehicles," Journal of Aerospace Computing, Information, and Communication, Vol. 3, No. 5, pp. 187-213, 2006.
35. Nonami, K., Kendoul, F., Suzuki, S., Wang, W., and Nakazawa, D., "Autonomous Flying Robots," Springer, 2010.

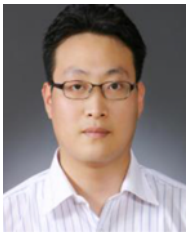

Min-Shik Roh

Ph.D. candidate in the Department of Aerospace Engineering, Pusan National University. His research interest is unmanned mobile system, avionic system, guidance and control.
E-mail: aeronobak@gmail.com

Beom-Soo Kang

He received his M.S. degree in aeronautical engineering from Korea Advanced Institute of Science and Technology, Korea in 1983. He received Ph.D. degree in mechanical engineering from University of California at Berkeley, at 1990. He joined Pusan National University as a Professor since 1993. His research interests include unmanned aerial vehicle system, computer-aided engineering of manufacturing process by finite element method for structural analysis, materials processing and metal forming.
E-mail: bskang@pusan.ac.kr